Surface distribution and depths profiling of particulate UV-absorbers by Raman imaging and tape stripping

Abstract

Tape-stripping in conjunction with scanning Raman microscopy was used for assessing the lateral and vertical distribution of an organic particulate UV-filter, MBBT (methylene bis-benzotriazolyl tetramethylbutylphenol) in a sunscreen formulation. 1 mg cm^{-2} formulation containing 10 % MBBT was applied on the volar forearms of three volunteers and the average amount of MBBT was measured by Raman scanning microscopy in 15 consecutive tape-strippings. The recovery of MBBT was 91.1 % with 30.2 % localizing on the skin surface (1^{st} strip), 42.5 % in the upper stratum corneum (strips 2 – 5) and from 3.6 down to 0.8 % in each of the 10 consecutive layers. The concentration of surface deposits of MBBT differed by a factor of 300 between folds, furrows, and pores on the one hand and the interjacent ridges on the other hand. 75 % of the applied particles occupied a fifth of the evaluated area – where concentrating in fold and furrows – as was confirmed by 3-D reconstruction. 8.6 % of MBBT distributed as very thin films preferentially on interjacent ridges. MBBT localized at sites not connected with the surface, such as in truncated pores or as potentially penetrated material amounted to 0.06 % or to twentieth of the 1.4 % found in the lowest skin strippings. Scanning Raman microscopy in combination with tape stripping documented the lateral and vertical distribution quantitatively and at cellular (12.5 µm) lateral resolution. Our results confirmed an earlier report on the vertical distribution of organic particles applied to skin and was in line with similar reports on TiO_2 distribution.

Introduction

Many sunscreen formulations contain as active principle poorly soluble nano- to micro-sized TiO_2 or ZnO particles, i.e. “physical sunscreens”. Recently, these inorganic particles have been complemented with a poorly soluble organic particulate UV-absorber, the micronized methylene bis-benzotriazoyl tetramethylbutylphenol (MBBT). Logic dictates that for their particulate nature physical sunscreens should protect the skin from ultraviolet radiation by forming a continuous film at the skins surface without penetrating to deeper layers of the stratum corneum as might chemical sunscreens, i.e. filter molecules dissolved in the sunscreen formulation. Indeed, investigations on the fate of particulate UV-filters performed mainly with TiO_2, the most abundantly used filter particle, confirmed this hypothesis: TiO_2 and MBBT-particles [1] concentrated at the skin surface and in the topmost layers of the stratum corneum. If at all, only isolated particles were found beyond the skin barrier, or detected particles were allocable to skin pores extending into the deeper regions, respectively [2].

In conjunction with the discussion on the safety of nano-sized materials applied onto skin, in vivo tape-stripping, in vitro skin penetration, various microscopy-based histological and in vivo confocal techniques have been suggested for monitoring particle distribution and penetration profiles [3]: On tape strips or in histological sections, inorganic particles are easily localized by their higher electron density and identified and quantified in situ via their elementary composition by means of X-ray fluorescence (XRF) [4], transmission electron microscopy (TEM) [5], proton induced X-ray emission (PIXE) [1,6], energy dispersive X-ray (SEM-EDX) [7,8] or by mapping the Ti-O-specific Raman signals of TiO_2 [2]. It is noteworthy that methods based on elementary composition do not apply for the analysis of organic particles in a biological or organo-chemical environment because the elementary compositions of the particles will be barely distinguishable from that of the surrounding skin, the thickeners and moisturizers in the topical sunscreen formulation, the composition of the tape and its adhesive or from the embedding resins of a histological section. Consequently, in order to profile the penetration of MBBT particles by serial tape stripping the MBBT was extracted with an appropriate solvent and then identified and quantified by HPLC [1]; however under loss of the lateral distribution of the particles.

In contrast to a compound's elementary composition obtainable via X-ray emission spectra (XRF, EDX, or PIXE) vibration spectroscopic techniques such as Raman or infrared spectroscopy provide specific information on the arrangement of atoms within a specific chemical molecule. Hence a particle's molecular constituents - if different from those in its environment - will display as distinct signals over a common background also in an environment constituted by the same elements. In turn, scanning confocal Raman microscopy has been employed recently for the assessment of the 1-D and 2-D distribution of specific organic molecules in a biological environment, such as mapping the distribution of carotenoids in human skin [9] the distribution of retinol [10], drugs [11] or of DMSO [12]. The vertical distribution of skin constituents and of water within human skin has been particularly well studied by confocal Raman microscopy [13-19].

In the following we document that scanning Raman microscopy in conjunction with tape-stripping can i) visualize the lateral distribution of organic micronized particles such as of MBBT on the skin surface, ii) document its 3-D distribution within the skin, and iii) concomitantly provide quantitative penetration profiles.

Material and Methods

Sunscreen formulation: The sunscreen formulation with 20 % Tinosorb™ M (50 % methylen bis-benzotriazolyl tetramethylbutylphenol (MBBT) in a dispersion of propylene glycol, decyl glucoside and xanthan gum) water, glyceryl stearate, PEG-100 stearate, C12-C15 alkyl benzoate, isopropyl palmitate, glycerin, dimethicone, steareth-10 allyl ether / acrylates copolymer, stearyl alcohol, tripalmitin, phenoxyethanol, methylparaben, butylparaben, ethylparaben, propylparaben, polysorbate-20 and sodium hydroxide, pH adjusted at pH = 6.5 and the placebo formulation without Tinosorb™ M were obtained from Ciba Inc., Basel, Switzerland.

Application of formulation on human skin: Excess abdominal skin – a gift from Spirig AG, Egerkingen, Switzerland – removed by plastic surgery was obtained under informed consent according to the Helsinki convention, prepared as split-thickness sheets and stored at -80 °C. A punch of a diameter of 12 mm was let to thaw at room temperature. 5 min later 1 mg cm^{-2} formulation was spread evenly on the skin surface with a glass rod. 30 min later the skin was mounted onto a metal disc loosely fitting into the cut-out of the Raman microscope's observation stage: the metal disc containing the skin was slightly pressed from below against a glass cover-slide (150 µm) glued onto the cut-out of the observation table, sealed with silicon-grease, and fixed mechanically from below with a spring holder. Raman spectra of the skin surface were registered through the cover glass, which was replaced for each skin sample.

Raman microscopy: Raman spectra (200-1800 cm^{-1}) of the skin sample were recorded by scanning an area of 4000 x 4000 um^2 with a lateral resolution of 14 µm thus acquiring a total of 80'000 spectra. Data were collected with a Renishaw inVia Reflex Raman microscope equipped with a StreamLine™ imaging system and a 1024 CCD detector (Renishaw plc, Wotton-under-Edge, GL12 8JR, UK) through a Leica EPI Plan 50x 0.75 NA objective by using a 532 nm laser for excitation. The average accumulation time for each spectrum was about 40 ms.

Data/Image analysis: The relative amount of MBBT was determined by the direct classical least square (DCLS) fitting routine of the instrument's WiRE™ 3.2 software using appropriate component

spectra of MBBT and of the stratum corneum and by applying a 3rd order polynomial background correction. The 2-D-image was constructed from the scores of the DCLS fits using MATLAB® 7.1 (MathWorks, 3 Apple Hill Drive, Natick, MA 01760 USA).

Application of the formulation on human volunteers: 1 mg cm^{-2} of sunscreen formulation was applied upon written consent onto the volar forearm of 3 volunteers (1 male, 2 females, aged 20 – 40 years). An area of 2 x 2 cm^2 was marked with a ballpoint pen on the volar forearm and approx. 4 mg of emulsion were evenly distributed across the test area and gently rubbed in with a small glass rod. The exact amount of formulation was determined by the weight of the glass rod before and after application of the sunscreen. Thereafter, the volunteers rested for 3 h at controlled laboratory conditions without covering the test area.

Tape stripping and Raman spectrosopy: The stratum corneum was removed layer-wise by tape stripping as described by Weigmann et al. [4]: In short, in total 15 layers of the stratum corneum were consecutively retrieved by adhesive tape (TESA film No. 5529, Beiersdorf, Hamburg, Germany, 19 mm). The tape strip was pressed onto the marked area by rolling it 10-times down with a roller. 10 seconds later, it was removed quickly and mounted with the sticky face up by double sided Scotch® adhesive tape onto a microscope slide. The procedure was then repeated with a new tape for stripping off the next layer. The removal of the 15 layers took approximately 15 minutes.

In the center of each tape strip an area of 5000 x 5000 μm^2 was scanned by recording a total of 160'000 Raman spectra (200-1800 cm^{-1}) with a lateral resolution of 12.5 µm and by defocussing an axial resolution of approx. 20 µm FWHM. The defocus corresponds to two times the 10 µm of stratum corneum reported to be removed by 15 strippings.[4, 17] To retrieve the consecutive strips from the very same site, the imprint of the tape covering the volar forearms at the outside of the analysed area served for positioning the microscope stage and coarsely aligning the subsequent strips to within 50 µm. The pixel to pixel alignment of the Raman images was done manually during data processing based on the bright field microscopic images.

Data/Image analysis: The relative amount of MBBT was obtained via DCLS fitting as described above for human skin by using the component spectra of MBBT, the stratum corneum and the tape's adhesive side. 2-D-images were constructed from the MBBT scores of the DCLS fits.

The absolute amount of MBBT was delineated from the average signal intensity of MBBT registered in an area reduced to 3760 x 3760 μm^2, i.e. to exclude boundary effects a 620 µm wide fringe zone was not considered. The size of the sampling area, i.e 3760x 3760 μm^2, used for collecting absolute data was judged for each tape strip as being representative by dividing the sampling area into 16 squares of equal size (940 x 940 μm^2) and determining the variation of the MBBT concentration given as standard error of the mean.

For calibration, the formulation was applied onto a microscopic slide as a film uniformly thinning-out from 56 µm to 0 µm tickness corresponding to a calculated change in MBBT concentration from 5.5 mg cm^{-2} to 0 mg cm^{-2}, respectively, and the film was allowed to dry. The change in intensity of the Raman signals registered for 818 points along the film proved linear with decreasing film thickness (R^2 = 0.9896). Component spectra of MBBT and the microscopic slide were used for the DCLS fits. By independent dilution experiments, the LOD for MBBT was determined as 0.02 %.

3-D-multivariate images were constructed from the 2-D-images by first stacking and aligning them manually and then visualizing the 3-D distribution using several MATLAB® programs. As a first estimate, the thickness of the retrieved skin was assumed to being the same in each strip.

All experiments were carried out in a controlled laboratory environment at 22 °C.

Results

Particle distribution visualized in vitro on human skin

To obtain a first impression of how MBBT-particles distribute on the skin surface, the MBBT containing sunscreen formulation was applied ex vivo to human split-skin and visualized by Raman microscopic mapping. The relative MBBT particle distribution reveals that most particles have arranged as a bright and interconnected network (Fig 1). A minor amount of MBBT particles is localized in between the network, where they form a continuous layer of weak spots extending over the whole scanned area. Such a distribution would agree with the particles concentrating in the skin's folds and furrows and additionally covering the interjacent ridges with a thin film.

Penetration of MBBT-particles assessed in three human volunteers by tape-stripping and quantified by scanning Raman microscopy

Penetration profiles for MBBT-particles were established from three volunteer (Fig 2) by retrieving the stratum corneum layers by tape-stripping three hours after topical application of a sunscreen formulation containing 10 % (w/w) of MBBT particles. MBBT-concentrations were determined on each of the 3 x 15 tape-strips by scanning Raman microscopy and then normalized to the amount of initially applied formulation, i.e. 1 mg cm^{-2} formulation corresponds to 100 %. The rate of recovery, i.e. the relative amount of MBBT retrieved from each volunteer by the 15 strippings, amounted to 98.4 ± 8.6 %, 101.3 ± 8.3 %, and 73.6 ± 6.8 %, or to an average recovery of 91.1 ± 9.2 % of the applied material, respectively. The relative amounts of MBBT recovered from each layer and the accumulated recovery by each stripping step are displayed in Fig 2. 30.2 % of the applied MBBT particles were localized at the skin surface by the first stripping. 42.5 % in the upper stratum corneum (strips 2 – 5) and from 3.6 down to 0.8 % in each of the 10 consecutive layers. The amount of MBBT recovered by subsequent stripping decreased essentially uniform with increasing depth to reaching 1.4 % after 15 strippings. The occasionally observed local increases (strips nine, eleven and fourteen) would be in accordance with the presence of truncated folds or pores.

Particle distribution visualized on the stratum corneum retrieved via tape-stripping

Surface, 1st strip, Raman image: The penetration of the MBBT-particles was quantified by tape-stripping as the average three volunteers (Fig. 2). The change of the lateral particle distribution with depth is illustrated for one individual in Fig. 3. The Raman mapping of the first strip provides an imprint of the MBBT-distribution on the skin surface three hours after application and prior to tape-stripping (Fig. 3a): A dense pattern of lengthy patches appears to be distributed at random. A closer look reveals additional smaller and less intense spots covering the space in between the lengthy patches and extending over the whole imaged area.

2nd strip, Raman image: Most of the smaller spots but not the distinct lengthy patches discernible in strips from the surface (Fig. 3a) are absent on the imprint obtained by the second stripping (Fig. 3b). Now the lengthy patches initially perceived to be oriented at random appear to be aligned in a distinct grid-like network. The emergence of a now well perceivable network on the second imprint concomitant with the disappearance of the interjacent fine spots would agree with the surface film covering the un-stripped surface being removed by the first tape-stripping, thus unveiling the MBBT-particles to concentrate preferentially in the skin's network of folds and furrows.

2nd strip, brightfield image: The conventional light micrograph of the 2nd tape strip (Fig. 3d) documents the stripped-off skin sticking to the tape strip: Flake-like structures (white circles) localize in between a grid-like network of narrow black and wider whitish structures spanning over the entire image, which is further divided by a sharp vertical line running parallel to the edge. The black network looks similar to its Raman-image displayed in Fig. 3b. This image would agree with corneocytes being removed preferentially from the skin ridges spared out by the network of folds and furrows. The finer black network would correspond to the distinct network of MBBT revealed by the Raman image (Fig. 3b) while the wider network would agree with a network of folds and furrows deeper and / or wider than the black-one and not filled to the rim with MBBT as the black-one. The often "crumbled" flakes decorating the wide network would also represent stripped off skin cells. The vertical line parallel to the image edge actually represents the edge of one of the two double-adhesive tapes used to fix the tape-strip on the microscopy slide.

15th strip, Raman-image: The fifteen tape-stripping from the volar forearm (Fig. 3d) corresponds to the removal of about 40 % of the stratum corneum [4], or based on Egawa et al. [17] to a depth of about 10 µm, respectively. In any case, only few particles are localized thus deep: Apart of the distinct spot accounting for more than 25 % of the detectable particles (arrow) some small isolated spots are perceivable. The position of the latter and of at least one of the bright spots seem to coincide with the MBBT-network displayed in Fig. 3b, which would indicate that these particles had not penetrated but are localized in skin folds or furrows extending beyond the last stripped-off layer. Particle-aggregates within skin pores would display alike as bright spots. Accordingly, of the MBBT-particles detected in this last strip and corresponding to about 1.4 % of the initially applied particles, at least half of the material may be allocated to structures extending further into the skin, i.e. the amount of particles having penetrated thus far can be assumed as half or less of those encountered.

Visualisation of overall MBBT distribution retrieved by tape-stripping

To illustrate the distribution of MBBT-particles within the stratum corneum, the absolute MBBT masses mapped by Raman in each of the 15 tape-strips were digitally aligned, overlaid, and processed pixel by pixel. Fig 4a shows the resulting density map for the total mass of MBBT accumulated over 15 tape-strips and detected in each of the 160'000 image points within the retrieved stratum corneum of one individual. Accordingly, the sunscreen formulation applied "evenly" to the skin had eventually distributed inhomogeneously with a high concentration of MBBT locating in presumed skin folds and furrows. Only a thin layer of MBBT was protecting the skin on top of the interjacent ridges.

3-D-reconstruction of lateral and vertical MBBT distribution

Lateral and vertical distribution of the MBBT was documented by reconstructing the 3-D distribution of MBBT from the mass data registered in a smaller area of 2500 x 2500 μm^2 or of 200 x 200 12.5 x12.5 μm^2 pixels,respectively, randomly selected from the absolute mass map data (Fig 4a). In turn, an arbitrary z-dimension corresponding to 1/15 of the maximal profile length was assigned to all pixels from this area. The resulting voxels were considered as loaded with MBBT if containing at

least 80 % of 1/15 of the MBBT/area initially applied, those containing less MBBT as empty. Profiles were then established by i) identifying the voxels located at corresponding sites in the 15 tape-strips and ii) by stacking them to its appropriate position (strip 1 – 15) in the resulting profiles. The thus reconstructed 3-D distribution of MBBT (Fig 4b) in the stratum corneum essentially follows the pattern of the highly concentrated MBBT in Fig 4a, confirming the presence of a network formed by folds and furrows. The majority of folds and furrows seemed to reach down to strips six to eight tape strips, i.e. to about five µm [4,17], a minority was extending down to strip 15 and possibly beyond.

Estimation of the maximal variation of film thickness

To have an idea of the variability of the film thickness the MBBT mass values corresponding to each of the 40'000 profiles registered in the selected area were attributed to quintile ranks Q1 to Q5, each quintile representing 20 % of the evaluated area (Fig 5a). Accordingly, the first three quintiles Q1 to Q3 representing 60 % of the evaluated skin, respectively, contained only 8.6 % of the recovered MBBT, while Q5, only 20 % of the evaluated skin, contained 75.1 % of the MBBT. In other words, 20 % (Q1) of the skin contained only 0.51 % of MBBT while another 20 % (Q5) contained 75.1 % of MBBT, i.e. the film thickness varied about 150-fold.

Areas/ structures represented by the different quintile ranks

The inserts of Fig 5a, Q1 to Q1-Q4, depict the localization of the profiles ranked accordingly, with white pixels standing for the presence, black pixels for the absence of profile sites. The profiles representing the lowest amounts of MBBT, i.e. those ranked in Q1, occupy sites interjacent or adjacent to a network of black patches and lines. Further addition of the profiles from Q2, Q3, and Q4 to the Q1-pool subsequently increased the presence of profile sites and reduced the black zones to a well-defined network devoid of MBBT (see Q1-Q4). This black network actually represents the not considered 75 % of MBBT contained in the profiles ranked in Q5. It is very similar to that of the MBBT-filled network of presumed folds and furrows documented in Fig 4 and of the overall profile pattern in the 3-D reconstruction displayed in Fig 4b and confirms the presence of a network of folds furrows and pores where MBBT preferentially accumulates.

Estimate of potentially penetrated MBBT particles in the individual tape strips.

With Q5 representing an essentially continuous network of MBBT in folds, furrows and pores, the remaining Q1 to Q4 represent smaller clusters and possibly single particles of MBBT essentially detached from the Q5-network and stemming also from truncated folds, furrows and pores or relating to penetrated material. In turn, the potentially penetrated material should be represented by the profiles ranked in Q1 to Q4, residing within these 80 % of skin. Therefore, each of the Q1 to Q4 profiles were searched for voxels having at least one voxel containing less or no MBBT stacked on top. As documented in Fig. 5b, cumulative values of the potentially penetrated MBBT accounted for 2.8 % in the second strip and declined to 0.06 % or ≤ 6 ng cm^{-2}, respectively, in strip fifteen.

Discussion

Since the lateral and vertical distribution of micro-sized particles such as inorganic TiO_2 or ZnO, and more recently the organic MBBT-particles may eventually affect the efficacy and safety of sunscreen, such particle containing formulations have been assessed with regard to particle distribution and particle penetration, the latter also in the context of “nano-safety”.[3,5,6,20-25] For this purpose, the stratum corneum is typically retrieved layer wise by tape stripping or is retrieved as a biopsy. Particles are then visualized by various microscopy techniques. Inorganic particles on tape-strippings or on histological sections from skin biopsies are usually identified via local elementary analysis often in combination with electron microscopy [1,2,7] or on skin biopsies in conjunction with serial sectioning and particle identification by electron microscopy [1,2,5,7,8,23-25].

Both, tape-stripping and sequential sectioning can provide a fair visual view of the lateral or vertical distribution of inorganic and organic particles. Yet, the quantification of organic particles is essentially restricted to providing penetration profiles relating to the total particles mass of the evaluated area without accounting for lateral particle distribution. This, because particles e.g. on tape strips have to be extracted and analyzed for their molecular composition, such as by HPLC. Their elementary composition usually based on X-ray spectroscopy would be barely discernible from that of the environment.

The present analysis is the first, to quantitatively access both the lateral and the vertical distribution of organic particles on skin. As illustrated in Fig 1, the scanning Raman microscopy image of a sunscreen formulation containing MBBT-particles applied to excised human skin represents in each image point the particle signals accumulated from the upper layers of the stratum corneum. Evidently, the MBBT particles are not distributed as a homogeneous film but their concentration follows the skin’s topography. The bulk of MBBT accumulates in the skin’s folds, furrows and pores, while only a thin film covers the ridges interjacent to this network. Such a distribution for TiO_2-particles has been observed in vivo based on TEM images of sections from biopsies, [1] and based on SEM-EDX images of tape strippings [7]. Moreover, both authors localized the bulk of

material within the topmost layers of the stratum corneum, be it via extraction of the tape strips and chemical analysis [1] or by micro-analysis of the tape strips for TiO_2 by SEM-EDX, respectively [7].

Scanning Raman microscopic assessment of MBBT distribution on tape stripping retrieved from three volunteers confirmed the vertical MBBT distribution reported by Mavon et al. [1]. The Raman-based average recovery of MBBT, i.e. 91.1 ± 9.2 %, is in good agreement with Mavon et al. who recovered an average of 92.2 % of MBBT in a similar study, yet extracting the strips and using HPLC for quantification. The same holds true for the vertical distribution: About a third of the MBBT was recovered from the skin surface and another third from the first layers of the stratum corneum, while the amount of MBBT localizing in the last strippings had evened out to a plateau of about 2 % (Fig 2), Such a constant amount of particles residing in deeper layers agrees with similar observations on TiO_2 [1,7] and MBBT [1] who attributed this remaining material as stemming from pores and deep furrows protruding 100 µm or further into the skin [7]. To this end, it maybe noteworthy that 15 tape strippings will remove roughly 10 µm [17] or 40 % [4] of the stratum corneum.

Scanning Raman microscopy registers for each lateral image point the local contribution of MBBT. Hence, a scanning Raman microscopic data set enclosing e.g. 15 strippings yields i) the quantitative lateral distribution of MBBT on each tape strip (Fig 3) and when strips are overlaid electronically ii) the 3-D mass distribution of MBBT-in the stripped-off skin volume. The importance of quantifying the lateral distribution is illustrated in Fig 3c. The distinct spot perceived in the last tape strip from one of the volunteers accounts for about 25 % of the MBBT in this strip (Fig 3c, arrows) or to 18 ng MBBT, respectively. One spot holding approximately 18 ng MBBT would account for a spherical particle with a diameter of 32 nm. Factually, the spot's position coincides with that of a strong furrow apparent on the 2nd tape strip of this stripping series (Fig 3b, arrow).

The 3-D Raman mass distribution map of MBBT (Fig. 4) allowed for i) estimating the average variability of local particle concentrations, ii) for displaying the 20 % of the image points representing 75.1 % of the MBBT mass in three dimensions (Fig. 5a) and for iii) estimating the maximal concentration of non-connected, i.e. of potentially penetrating MBBT (Fig. 5b). In

accordance with others [7] the applied formulation varied substantially, i.e. here in the range of 150-fold, between the surface area and the folds and furrows. The image points representing the highest quintile rank manifested as an essentially interconnected network concentrating in the upper levels and occasionally with profiles reaching down to lower strips (Fig. 4b). A key feature of penetrating entities is that their vertical profile does not connect to the surface. In turn, MBBT accumulation of non-continuous profiles should give the maximal level of potentially penetrating particles, i.e. maximal because truncated or ingrown pores, and particle-clusters below the surface etc. were included. This maximal amount of potentially penetrating particles reached 0.06 % or 6 ng cm^{-2} respectively, hence values in the scatter of analytical sensitivity and comparable to other reports referring essentially to the absence of particle penetration [1,2,7].

Conclusion

As exemplified by evaluating the distribution of topically applied MBBT on skin, tape-stripping which is regarded as non- or least-invasive [4,26,27] in conjunction with scanning Raman microscopy provides the quantitative lateral and vertical distribution of organic moieties in the epidermis, i.e. in an in vivo environment and with cellular (sic 12.5 x12.5 μm^2) resolution. Scanning Raman microscopy allows for 3-D-imaging and quantification especially in cases i) where the molecule of interest exhibits a similar elementary composition as its environment, as is the case with organic moieties embedded in a formulation of similar chemical composition or applied to skin and ii) where the lateral and vertical distribution of organic moieties should be quantified and resolved at cellular resolution. Moreover, the use of tape-stripping in conjunction with scanning Raman microscopy is not only confined to tracing skin penetration of particles. It has the potential to reveal in a more general sense 3-D penetration patterns of any topically applied formulation, be it with respect to i) drug penetration or to ii) differing penetration behavior of a topical formulation's constituents, and this at microvascular or even cellular resolution.

References

1. Mavon, A., Miquel, C., Lejeune, O., Payre, B. and Moretto, P. In vitro percutaneous absorption and in vivo stratum corneum distribution of an organic and a mineral sunscreen. *Skin Pharmacol. Physiol.* 20,10-20 (2007).

2. Lademann, J., Weigmann, H., Rickmeyer, C., Barthelmes, H., Schaefer, H., Mueller, G. and Sterry, W. Penetration of titanium dioxide microparticles in a sunscreen formulation into the horny layer and the follicular orifice. *Skin Pharmacol. Appl. Skin Physiol.* 12, 247-256 (1999).

3. Warheit, D.B., Borm, P.J., Hennes, C. and Lademann, J. Testing strategies to establish the safety of nanomaterials: conclusions of an ECETOC workshop. *Inhal. Toxicol.* 19, 631-643 (2007).

4. Weigmann, H.-J., Lademann, J., Meffert, H., Schaefer, H. and Sterry, W. Determination of the Horny Layer Profile by Tape Stripping in Combination with Optical Spectroscopy in the Visible Range as a Prerequisite to Quantify Percutaneous Absorption. *Skin Pharmacol. Appl. Skin Physiol.* 12, 34-45 (1999).

5. Schulz, J., Hohenberg, H., Pflücker, F., Gärtner, E., Will, T., Pfeiffer, S., Wepf, R., Wendel, V., Gers-Barlag, H. and Wittern, K.P. Distribution of sunscreens on skin. *Adv. Drug Deliv. Rev. 54 Suppl.* 1, S157-S163 (2002).

6. Menzel, F., Reinert, T., Vogt, J. and Butz, T. Investigations of percutaneous uptake of ultrafine TiO_2 particles at the high energy ion nanoprobe LIPSION. *Nucl. Instr. Meth. B* 219/220, 82-86 (2004).

7. Pflücker, F., Hohenberg, H., Hölzle, E., Will, T., Pfeiffer, S., Wepf, R., Diembeck, W., Wenck, H. and Gers-Barlag, H. The Outermost Stratum Corneum Layer is an Effective Barrier Against Dermal Uptake of Topically Applied Micronized Titanium Dioxide. *Int. J. Cosmet. Sci.* 21, 399-411 (1999).

8. Senzui, M., Tamura, T., Miura, K., Ikarashi, Y., Watanabe, Y. and Fujii, M. Study on penetration of titanium dioxide (TiO_2) nanoparticles into intact and damaged skin in vitro. *J. Toxicol. Sci.* 35, 107-113 (2010).

9. Darvin, M.E., Fluhr, J.W., Caspers, P., van der Pol, A., Richter, H., Patzelt, A., Sterry, W. and Lademann, J. In vivo distribution of carotenoids in different anatomical locations of human skin: comparative assessment with two different Raman spectroscopy methods. *Exp. Dermatol.* 18, 1060-1063 (2009).

10. Pudney, P.D., Mélot, M., Caspers, P.J., van der Pol, A. and Puppels, G.J. An in vivo confocal Raman study of the delivery of trans retinol to the skin. *Appl. Spectrosc.* 61, 804-811 (2007).

11. Tfayli, A., Piot, O., Pitre, F. and Manfait, M., Follow-up of drug permeation through excised human skin with confocal Raman microspectroscopy. *Eur. Biophys. J.* 36, 1049-1058 (2007).

12. Zhang, G., Moore, D. J., Flach, C. R. and Mendelsohn, R. Vibrational microscopy and imaging of skin: from single cells to intact tissue. *Anal. Bioanal. Chem.* 387, 1591-1599 (2007).

13. Caspers, P.J., Lucassen, G.W., Carter, E.A., Bruining, H.A. and Puppels, G.J. In vivo confocal Raman microspectroscopy of the skin: noninvasive determination of molecular concentration profiles. *J. Invest. Dermatol.* 116, 434-442 (2001).

14. Caspers, P. J., Lucassen, G. W., Wolthuis, R., Bruining, H. A. and Puppels, G. J. In vitro and in vivo Raman spectroscopy of human skin, *Biospectroscopy* 4, S31-S39 (1998).

15. Bielfeldt, S., Schoder, V., Ely, U., van der Pol, A., de Sterke, J. and Wilhelm, K.-P. Assessment of human stratum corneum thickness and its barrier properties by in-vivo confocal Raman spectroscopy. *IFSCC Magazine* 12, 9-15 (2009).

16. Caspers, P.J., Lucassen, G.W. and Puppels, G.J. Combined in vivo confocal Raman spectroscopy and confocal microscopy of human skin. *Biophys. J.* 85, 572-580 (2003).

17. Egawa, M., Hirao, T. and Takahashi, M. In vivo estimation of stratum corneum thickness from water concentration profiles obtained with Raman spectroscopy. *Acta Derm. Venereol.* 87, 4-8 (2007).

18. Nakagawa, N., Matsumoto and M., Sakai, S. In vivo measurement of the water content in the dermis by confocal Raman spectroscopy. *Skin Res. Technol.* 16, 137-141, (2010).

19. Tfayli, A., Piot, O. and Manfait, M. Confocal Raman microspectroscopy on excised human skin: uncertainties in depth profiling and mathematical correction applied to dermatological drug permeation. *J. Biophotonics* 1, 140-153 (2008).

20. Schneider, M., Stracke, F., Hansen, S. and Schaefer, U. F. Nanoparticles and their interactions with the dermal barrier. *Dermatoendocrinol.* 1, 197-206 (2009).

21. Wokovich, A., Tyner, K., Doub, W., Sadrieh, N. and Buhse, L.F. Particle size determination of sunscreens formulated with various forms of titanium dioxide. *Drug Dev. Ind. Pharm.* 35, 1180-1189, (2009).

22. Sadrieh, N., Wokovich, A.M., Gopee, N.V., Zheng, J., Haines, D., Parmiter, D., Siitonen, P.H., Cozart, C.R., Patri, A.K., McNeil, S.E., Howard, P.C., Doub, W.H. and Buhse L.F. Lack of Significant Dermal Penetration of Titanium Dioxide (TiO_2) from Sunscreen Formulations containing Nano- and Sub-Micron-Size TiO_2 Particles. *Toxicol. Sci.* 115, 156-166 (2010).

23. Filipe, P., Silva, J.N., Silva, R., Cirne de Castro, J.L., Marques Gomes, M., Alves, L.C., Santus, R. and Pinheiro, T. Stratum corneum is an effective barrier to TiO2 and ZnO nanoparticle percutaneous absorption. *Skin Pharmacol. Physiol.* 22, 266-275 (2009).

24. Wu, J., Liu, W., Xue, C., Zhou, S., Lan, F., Bi, L., Xu, H., Yang, X. and Zeng F.D. Toxicity and penetration of TiO_2 nanoparticles in hairless mice and porcine skin after subchronic dermal exposure *Toxicol. Lett.* 191, 1-8 (2009).

25. Newman, M.D., Stotland, M. and Ellis, J.I. The safety of nanosized particles in titanium dioxide- and zinc oxide-based sunscreens. *J. Am. Acad. Dermatol.* 61, 685-692 (2009).

26. Escobar-Chávez, J.J., Merino-Sanjuán, V., López-Cervantes, M., Urban-Morlan, Z., Piñón-Segundo, E., Quintanar-Guerrero, D. and Ganem-Quintanar, A. The tape-stripping technique as a method for drug quantification in skin. *J. Pharm. Pharm. Sci.* 11, 104-130 (2008).

27. Darlenski, R., Sassning, S., Tsankov, N., Fluhr, J.W. Non-invasive in vivo methods for investigation of the skin barrier physical properties. *Eur. J. Pharm. Biopharm.* 72, 295-303 (2009).
y facilities.

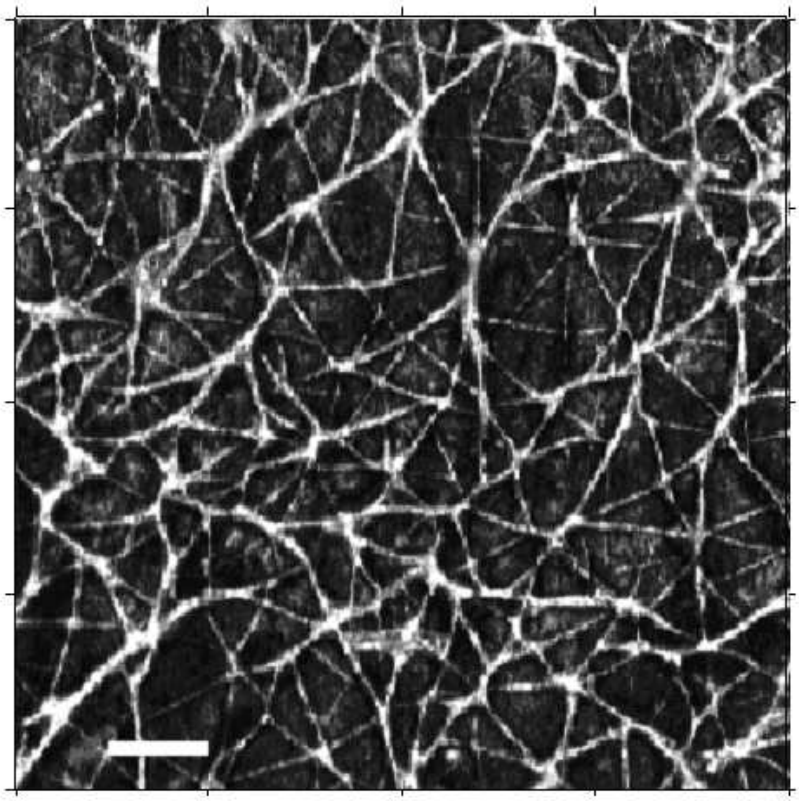

Figure 1: Distribution of the particulate UV-filter MBBT on excised human skin. The MBBT map is obtained from the scattered Raman signals by operating a defocused 532 nm laser for excitation to a depth of 20 µm. Scale bar 500 µm.

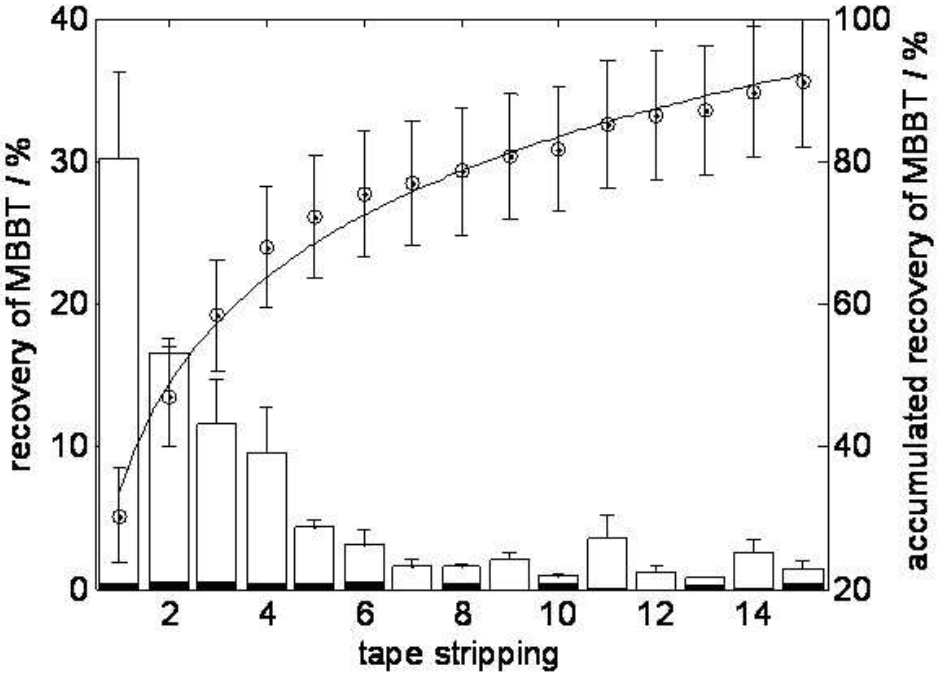

Figure 2: MBBT retrieved by 15 tape strippings from three volunteers three hous after application of 1 mg cm-2 sunscreen formulation containing 10 % MBBT to the volar forearm. The MBBT was quantified on each strip by scanning Raman microscopy. Recovery: 91.1± 9.2 % of the applied amount. Left ordinate, white columns: Average recovery by each tape stirpping, Error bars: standard error of the mean, S. E. M., n = 3. Black columns: placebo control (single volunteer). Right ordinate, circles: Amount of MBBT accumulated by consecutive stripping. Error bars: S. E. M. with consideration of error propagation.

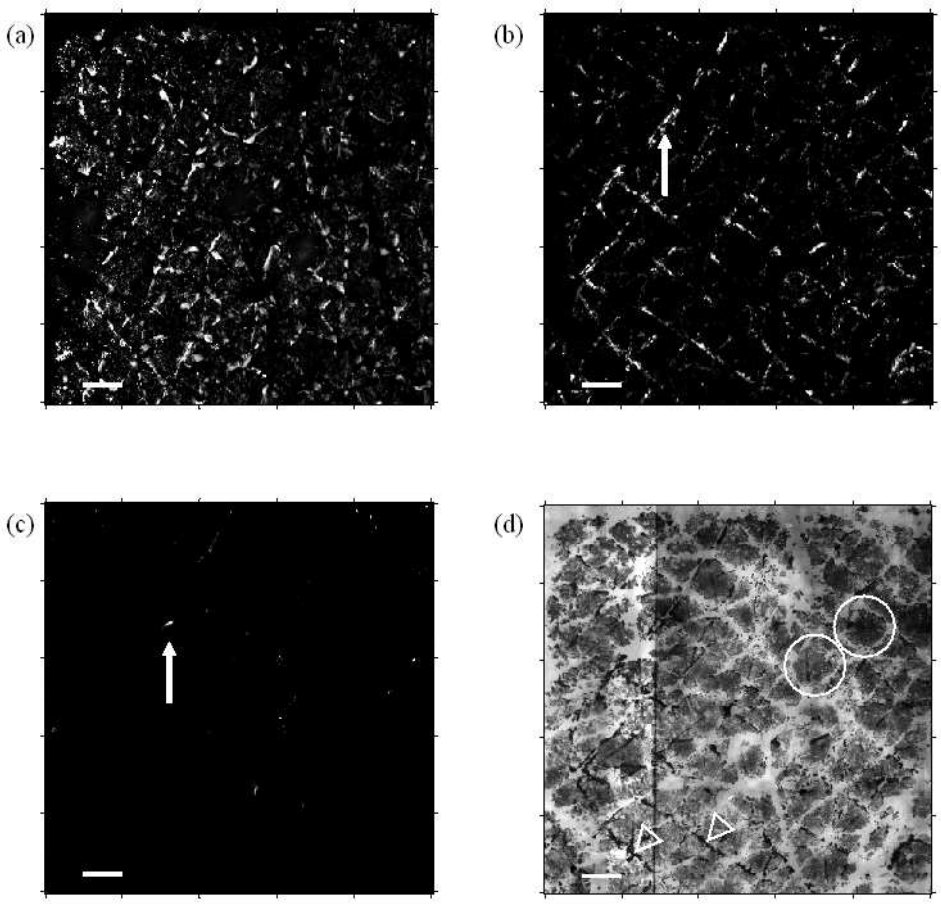

Figure 3: MBBT distribution on individual tape strippings. Scanning Raman microscopy maps. The MBBT mass is represented by the intensity of white (black = no mass).
3a: 1st tape strip: Rip-off of the formulation on the skin's surface 3 h after topical application.
3b: 2nd tape strip: Rip-off of the first layer from the stratum corneum. Note the presence of network-like distributed MBBT (skin furrows) as in the 1st tape strip, yet in absence of interjacent MBBT.
3c: 15th tape strip: MBBT is practically absent: The spot accounting for > 25 % of the total MBBT in this strip (arrow) collocates with a furrow (arrow, 3b)
3d: Conventional light micrograph of 2nd tape strip. Note the flake-like cells (white circles) and further ripped-off material (white triangles) essentially following the MBBT network displayed in 3b.
Scale bar 500 µm.
206x199mm (96 x 96 DPI)

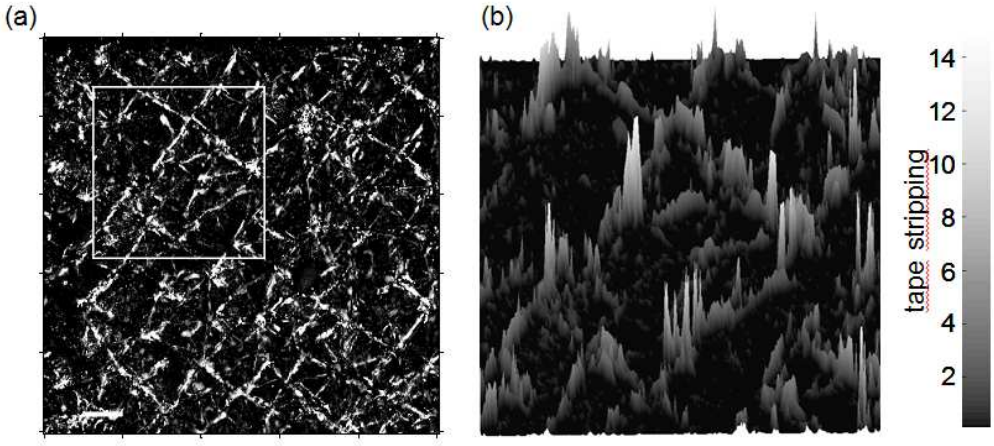

Figure 4: 3-D map of MBBT mass distribution obtained by aligning and overlaying the scanning Raman microscopy mass maps for MBBT of each of the 15 tape strips.
4a: Accumulated MBBT mass (white) distributed within a 5000 x 5000 µm2 area in the centre of the overlaid tape strips. Zones without MBBT: black. Scale bar 500 µm.
4b: 3-D reconstruction of vertical and lateral distribution of MBBT within a randomly selected area (4a). Mass profiles were established by i) assigning to each of the 40'000 registered 12.5 x 12.5 µm2 image points (pixels) an arbitrary z-dimension of 1/15 of the maximal profile depths and by stacking the resulting voxels of each tape strip to the corresponding profiles. Note that the deeper profiles containing a major amount of MBBT collocate with the network of presumed skin folds and furrows displayed in 4a.

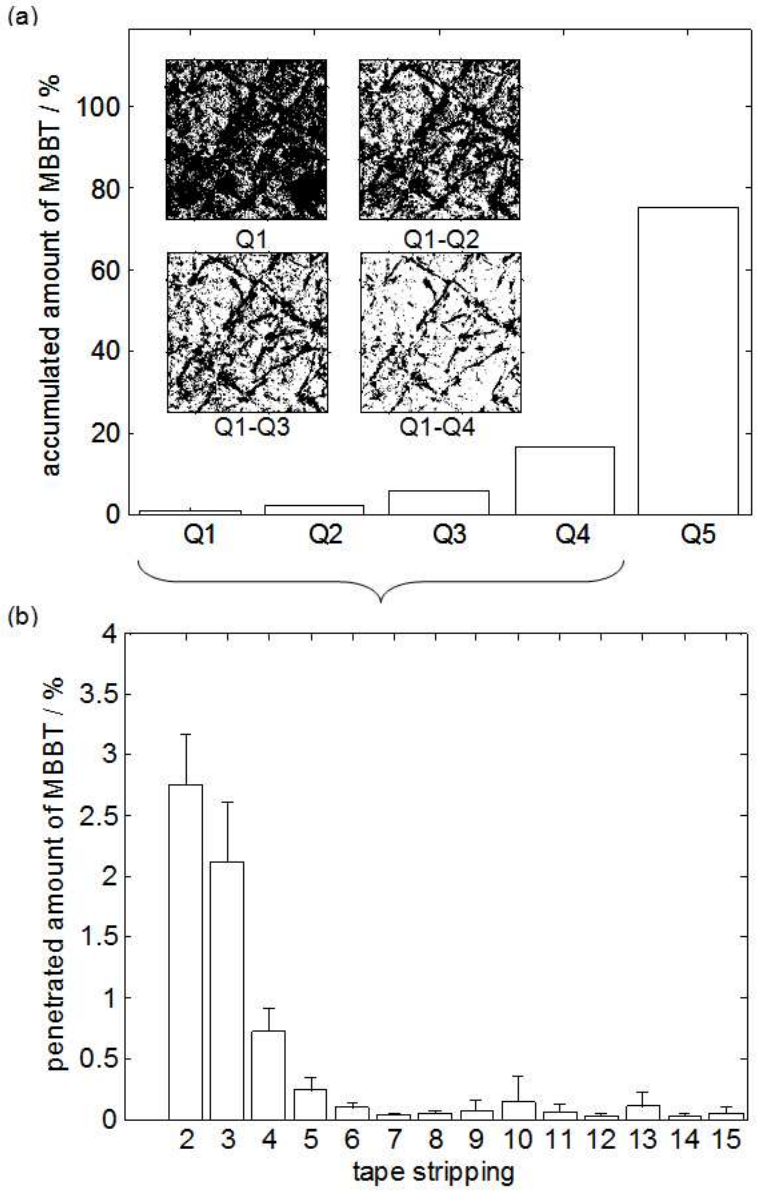

Figure 5: Estimation of the maximal variation of film thickness and of potentially penetrated particles by quintile ranking of the MBBT mass profiles

Fig 5a: Quintile ranking of the 40'000 density profiles registered for 3-D-reconstruction (Fig. 4b). The four inserts locate the sites of the MBBT mass profiles (white) corresponding to the respective ranks. Note, the lowest ranked profiles (Q1) locating essentially interjacent and adjacent to the network of patches and lines with MBBT (black). The black network in Q1-Q4 corresponding to the network of furrows in 4a (inserted square) actually represents the missing profiles of Q5. The average MBBT concentration accumulated in Q1 and Q5 varies by about 150-fold.